Food Analytical Methods
https://doi.org/10.1007/s12161-018-1323-x

Integrated Analytical Methods to Characterize Lipids from *Prosopis* spp. and *Ceratonia siliqua* Seed Germ Flour

Francesco Siano[1] · Leonardo Sciammaro[2] · Maria Grazia Volpe[1] · Gianfranco Mamone[1] · Maria Cecilia Puppo[2] · Gianluca Picariello[1]

Received: 17 April 2018 / Accepted: 2 July 2018

Abstract
Flour from seed germ of European carob (*Ceratonia siliqua*) and South American algarrobo (*Prosopis* spp.) is a potential ingredient for health-promoting baked products. Herein, lipids from germ of three Argentinean *Prosopis* (*P. alba*, *P. nigra*, and *P. ruscifolia*) and one European carob species were characterized in detail, exploiting an array of up-to-date analytical techniques. Total lipids ranged from 7.1 to 8.1% (*w*/*w*). Linoleic acid (C18:2, ω-6) predominated the GC flame ionization detector profiles of fatty acid in all samples (43.3–50.6%). *Prosopis* spp. contained 6–7% of C20–C24 fatty acids and, consistently, C56–C60 triacylglycerols, as detected by MALDI-TOF mass spectrometry (MS), which were practically missing in *C. siliqua* germ. Phospholipids were isolated by hydroxyapatite chromatography, characterized by MALDI-TOF MS and grossly quantified by attenuated total reflectance Fourier transform infrared (ATR-FTIR) spectroscopy. Because of a relatively high content (9.5–11.8%, *v*/*v*), phospholipids might increase the antioxidant potential and improve the baking performances of flour fortified with carob and algarrobo seed germ.

Keywords *Ceratonia siliqua* · *Prosopis* spp. · Seed germ lipids · GC-FID · MALDI-TOF MS · ATR-FTIR

Introduction

Carob powder, obtained from pods of Mediterranean *Ceratonia siliqua* L., is a natural sweetener with flavor and appearance similar to chocolate. Because of a high content of bioactive compounds, it has been traditionally used and recently revalued as a cocoa substitute with the advantage that it is free from caffeine and theobromine. Both *C. siliqua* and South American algarrobo (*Prosopis* spp.) belong to the *Leguminosae* family, thus sharing many morphological and compositional traits. Similar to carob, the flour obtained from pods of *Prosopis* spp. is brown and sweet and has a taste and aroma with hints of coffee, cocoa, coconut, and hazelnut. Native to South America, *Prosopis* trees and shrubs have been widely distributed in the semiarid regions of Africa and Asia, as they could be multipurpose valuable resources, including human nutrition (Choge et al. 2007).

C. siliqua and *Prosopis* spp. flours constitute ingredients of high nutritional value, because of components with health-promoting properties, such as polyphenols, which are mainly located in the pod exocarp, lipids and proteins also present in seeds (Ayaz et al. 2007; Custódio et al. 2011; Pérez et al. 2014; Sciammaro 2015). The absence of gluten-like prolamins is the key for the increasing use of these flours as food ingredients in gluten-free baked products.

Seeds of both *Prosopis* spp. and *C. siliqua* comprise 10–15% in weight of the pod and contain a gummy endosperm, which, at least in the case of Mediterranean carob, is already largely used by food industry as a texturing and thickening agent (locust bean gum). Germ accounts for almost the half of the seed weight and is a by-product remaining after removal of seed cuticle and inner gum layer (Sciammaro et al. 2016). The flour obtained from *C. siliqua* and *Prosopis* seed germ is relatively rich in high-biological value proteins and has been proposed as an ingredient able to enhance the protein content of baking flours (Saunders and Becker 1989). Preliminary

✉ Maria Cecilia Puppo
mcpuppo@quimica.unlp.edu.ar

✉ Gianluca Picariello
picariello@isa.cnr.it

[1] Istituto di Scienze dell'Alimentazione, Consiglio Nazionale delle Ricerche (CNR), Via Roma 64, 83100 Avellino, Italy

[2] Centro de Investigación y Desarrollo en Criotecnología de Alimentos (CIDCA – UNLP – CONICET), Calle 47 y 116, 1900 La Plata, Argentina

Published online: 14 July 2018

determinations indicate that *Prosopis* spp. germ proteins have solubility, whipping, and emulsifying properties comparable to soy protein isolate, with the additional advantage of being most likely not allergenic (Saunders and Becker 1989).

Seed germs from both *Prosopis alba* and *C. siliqua* contain potential bioactive properties, in particular related to apigenin C-glycosides as the main polyphenol constituents (Batista and Gomez 1993; Cattaneo et al. 2016). Very recently, isoschaftoside and schaftoside have been characterized as the most abundant phenolic compounds in the germ from three species of *Prosopis* (namely, *P. alba*, *P. nigra*, and *P. ruscifolia*) and *C. siliqua* (3.22–5.18 and 0.41–0.72 mg/g of germ flour, respectively), occurring along with other C-glycosylated apigenin derivatives (Picariello et al. 2017). Interestingly, apigenin C-glycosides are potent inhibitors of α-glucosidases in vitro (Li et al. 2009). Therefore, they might delay the digestion of starchy foods in vivo and are candidate phytochemicals to prevent or to treat type 2 diabetes. Several attempts of producing wheat-free pasta or baked products using either pure or combined carob germ flour have been already described since decades. The most interesting results concern the preparation of high-protein foods for diabetics (Smith et al. 2010).

In general, polyphenols primarily contribute to the antioxidant activity of a food ingredient.

There is evidence that not only polyphenols but also other classes of compounds, such as lipids, would contribute to this effect. Indeed, Sciammaro et al. (2016) found that antioxidant activity of *P. alba* seeds, which is lower in polyphenol compared to other species, was approximately three times greater than that detected in pod flour, most likely depending at least in part on the higher lipid content of the seed germ.

Lamarque et al. (1994) reported 12.7% of lipids in *P. alba* seeds, with a composition of 27.6 and 52.5% of oleic and linoleic acids, respectively. In preliminary experiments, 14 fatty acids (FAs) were identified in germs of *P. alba* and *P. nigra*, being linoleic the predominant FA accounting for 44.6 and 47.7%, respectively (Sciammaro 2015). Oleic acid ranked the second most abundant FA, with values of 26.5 and 25.7%, respectively. On the other hand, Avallone et al. (1997) reported values significantly different from other investigators, with a total lipid content of 0.4, 2.8, and 1.1% for pod, germ, and seed of *C. siliqua*, respectively. Dakia et al. (2007) determined a total lipid content of 6.6% in seeds of *C. siliqua*, which included 21% of polar lipids such as phospholipids, diglycerides, monoglycerides, and probably glycolipids, the latter very recently confirmed in germ (Picariello et al. 2017). Oleic (34.4%) and linoleic (44.5%) acids were the major FAs, while palmitic (16.2%) and stearic (3.4%) acids were the main saturated ones. Thus, from this survey, it appears clear that available data about the lipid composition of *C. siliqua* and *Prosopis* spp. seed germ are fragmentary and, in some instances, controversial.

Certainly, carob and algarrobo seed germ oil is a good source of polyunsaturated FA (ω-6), which can contribute to maintain a healthy state in humans and to ameliorate pathological conditions such as growth retardation (Dakia 2011).

In this work, an array of analytical techniques was exploited to comparatively characterize the lipid classes from seed germ of some species of *Prosopis* most commonly used for human alimentary purposes and from the *C. siliqua* counterpart. In particular, phytosterols and phospholipids have been analyzed for the first time at a molecular level, to the best of our knowledge. Such information is particularly relevant in the perspective of using carob and algarrobo seed germ on a large scale as an ingredient for the preparation of high-quality baked commodities and other food products with potential health-promoting benefits.

Materials and Methods

Materials

HPLC grade solvents, including chloroform, methanol, acetonitrile, and *n*-hexane, were purchased from Carlo Erba (Milan, Italy). All the chemicals were from Sigma-Aldrich (St. Louis, MO, USA).

Algarrobo and Carob Seed Germ Flour Samples

Prosopis (*P. alba*, *P. nigra*, and *P. ruscifolia*) pods were collected in Santiago del Estero (Argentina) between 2010 and 2014. Seeds were hulled from pods, soaked in boiling water for 10 min, and then cooled and rested overnight at 4 °C, in order to allow swelling of the different seed compartments. Epicarp, endosperm, and germ from *Prosopis* spp. seeds were manually separated, in particular to release the germ from the gum envelope (Sciammaro et al. 2016). Isolated germ specimens was freeze-dried, ground into a fine flour (seed germ flour, SGF), and stored at − 20 °C until used. Approximately 200 g of germ flour was obtained for each species, which was representative of the seeds collected over 5 years. European carob (*Ceratonia siliqua*) seed germ flour was supplied by Pevesa Biotech (Spain).

Total Lipid Extraction

Total lipid fraction of SGF was extracted with the Bligh and Dyer method, according to Bahrami et al. (2014). Briefly, 500-mg aliquots of SGF was suspended in water (1 mL) to produce a wet slurry to which 3.75 mL chloroform/methanol (1:2, *v*/*v*), 1.25 mL chloroform, and 1.25 mL water were sequentially added. Between each solvent addition, the mixture was vigorously vortexed for 10 min and, at the end, centrifuged (3.500×*g*, 4 °C, 15 min). The lower phase was collected,

and the interfacial pellet was re-extracted using the same procedure. The organic layers were finally combined and dried under a N_2 stream.

GC Flame Ionization Detector Analysis of FAME and Unsaponifiable Fraction

Analysis of the fatty acid methyl esters (FAMEs) was performed according to the AOAC Official Method 996.0.20 (Association of Official Analytical Chemists (AOAC) 2001). FAMEs were obtained through direct hydrolysis/methylation carried out on 500-mg SGF aliquots, which were suspended in 2 mL of 1.25 N HCl/CH_3OH solution in Pyrex test tubes with screw caps and incubated in a water bath at 90 °C for 60 min. After the addition of 2 mL of deionized water, FAMEs were extracted with *n*-hexane and filtered using Millex 0.45-μm PVDF disposable syringe filters (EMD Millipore Corp., Billerica, MA, USA). Analyses were carried out with a Trace GC gas chromatograph (Thermo Scientific, Inc., San Jose, CA, USA) equipped with a flame ionization detector (FID), using an SP-2560, 100 m × 0.25 mm × 0.20 μm capillary column (Supelco-Sigma-Aldrich). FAME extracts (1 μL) were introduced through a split-splitless injection system of an AS 3000 autosampler in split mode (ratio 1:100) at 260 °C and analyzed as previously detailed (Siano et al. 2016). FA composition of SGF was obtained by comparison with the retention times of the standard mixture FAME 37 components (Sigma) and was expressed as a percentage area.

After the addition of 5-α-cholestan (Sigma) as the internal standard, SGF lipid extracts were saponified and analyzed according to Caligiani et al. (2010). Briefly, the unsaponified components were extracted in diethyl ether and washed with water until neutral reaction. Ether phase was dehydrated with anhydrous sodium sulfate, filtered on paper, and finally dried under vacuum. The oil residue was dissolved in 50 mL of *n*-hexane and analyzed using the above chromatograph equipped with a RTX-5, 30 m × 0.25 mm × 0.25 μm column (Restek, Bellefonte, PA, USA). Samples (1 μL) were introduced through the autosampler in 1:10 split mode at 250 °C. The oven temperature program started at 200 °C (held for 2 min) and linearly increased to 300 °C (20 °C/min) at the end of the analysis. Plant sterol mix (Matreya, State College, PA, USA) containing brassicasterol (13%), campesterol (26%), stigmasterol (7%), and β-sitosterol (53%), together with squalene and α- and γ-tocopherols, (Sigma) was used as an external standard for qualitative and quantitative determinations. External calibration curves were built for both sterols of the standard mix and remaining individual analytes. Due to the unavailability of the corresponding standard, Δ_5-avenasterol was tentatively assigned by comparison with published GC chromatograms (Phillips et al. 2005) and semiquantified based on the internal standard peak area. Data were recorded and processed using the ChromQuest 5.0 software (Thermo). GC runs were performed in triplicate at least (technical replicates). Values are reported as the mean of three determinations and relative standard deviation, calculated using SigmaPlot ver. 12.5.

Triacylglycerol and Phospholipid Separation

Neutral lipids and phospholipids were fractionated using the ceramic hydroxyapatite (HAP) methods previously described (Pinto et al. 2014). To this end, nearly one fifth of the total lipid extracts from 500 mg SGF was suspended in 0.5 chloroform and transferred in a clean glass tube containing 30 mg of ceramic HAP (Macro-Prep Ceramic CHT-Type I, 40 μm particle diameter; Bio-Rad, Berkeley, CA, USA). After 5 min of soft agitation, the suspension was centrifuged (2500×*g*, 15 °C, 2 min). The HAP beads were then sequentially incubated with 0.5 mL of $CHCl_3$ and 0.5 mL of $CHCl_3/CH_3OH$ (2:1, *v*/*v*). The supernatants from the three steps were combined and saved as the flow-through. Finally, phospholipids (PLs) were recovered in the supernatants produced through vigorous agitation of HAP beads suspended in 0.5 mL of a $CHCl_3$/CH_3OH/1 M sodium phosphate, pH 7.2 (6:3:1, *v*/*v*/*v*), ternary mixture and subsequent centrifugation.

MALDI-TOF MS

Prior to MS analysis, 5 μL of a 1 mg/mL $CHCl_3/CH_3OH$ (2:1, *v*/*v*) solution of the total lipid extracts was diluted in 1 mL of $CHCl_3$ and vigorously vortexed with 1 mL of 0.5 M aqueous sodium acetate in order to promote the ionization of triacylglycerols (TAGs) exclusively as Na^+ adducts. After separation of the biphasic system, the organic layer was used for the analysis. MALDI-TOF mass spectra were acquired on a Voyager-DE PRO (PerSeptive Biosystems, Framingham, MA, USA), as previously described (Pinto et al. 2014). Experiments were performed in the reflector positive ion mode using 10 mg/mL 2,5-dihydroxybenzoic acid (DHB) in 50% aqueous acetonitrile (*v*/*v*) containing 5 mM sodium acetate as the matrix. External mass calibration was performed with a separate acquisition of standard TAG (obtained from Sigma-Aldrich). Analyses were carried out in triplicate to check for the repeatability. Mass spectra were elaborated and compared using the Data Explorer 4.0 software (PerSeptive Biosystems). Individual PL fractions were analyzed using the same conditions of TAG, except that the cationization step was skipped. In this case, the HAP eluate (1 μL) was mixed with 1 μL of the matrix directly onto the stainless steel target plate (PerSeptive Biosystems) and was air-dried prior to analysis. PL fractions were additionally analyzed in the reflector negative ion mode using 9-aminoacridine (10 mg/mL in isopropanol/acetonitrile 60:40, *v*/*v*) as the matrix (Fuchs et al. 2009).

Attenuated Total Reflectance Fourier Transform Infrared Spectroscopy

Attenuated total reflectance Fourier transform infrared (ATR-FTIR) analyses were performed using a Spectrum 400 spectrophotometer (PerkinElmer, Waltham, MA USA), equipped with a deuterated triglycine sulfate (DTGS) detector. Lipid extracts were dissolved in $CHCl_3$, and a drop of the resulting solution was spotted onto the ATR diamond crystal. After solvent evaporation, 32 scans/spectrum were acquired in the 4000–650 cm^{-1} range with a resolution of 4 cm^{-1}. Characteristic PL bands were singled out using 8 mg/mL of standard phosphatidylcholine (PC; Sigma) in $CHCl_3$. To quantify PL in the presence of co-extracted TAG, a calibration curve was generated by mixing two equimolar solutions of standard PC and triolein (Fluka, Seelze, Germany) at varying relative concentrations (PC/triolein, 1, 5, 10, 20, and 50%, *v*/*v*). Spectra were elaborated using the PerkinElmer Spectrum software (version 10.5.1), purchased with the instrument. Samples were analyzed without any previous treatment. To check for repeatability, analyses were performed in triplicate and average spectra were used. The method was validated using a lipid extract of egg yolk, with approximately known total PL concentration (28% PL of the lipid fraction, *w*/*w*).

Results and Discussion

Total Lipid Content

Total lipid content was estimated by gravimetric analysis. It was 7.4, 7.6, and 8.1% (*w*/*w*) for SFG of *P. alba*, *P. nigra*, and *P. ruscifolia*, respectively, while SFG of *C. siliqua* exhibited a slightly lower amount corresponding to 7.1% (*w*/*w*). The current determination was in good agreement with the total lipid content of *C. siliqua* germ previously reported (Dakia et al. 2007).

Fatty Acids of SGF

The GC-FID chromatograms of FAME generated by direct methylation of *Prosopis* spp. and *C. siliqua* SGF are compared in Fig. 1. Linoleic acid (C18:2, ω-6) was the predominant FA, with values ranging between 43.3% in *C. siliqua* and 50.6% in *P. alba* (Table 1). Oleic acid (C18:1, ω-9) also occurred at relatively high levels ranging between 21.2% in *P. alba* and 32.0% in *C. siliqua*. The most abundant saturated FA in SGF samples was palmitic acid (C16:0), accounting for less than 15% in all the samples. The FA composition determined in this work was in very close agreement with that of previous determinations of lipids from *C. siliqua* (Dakia et al. 2007) and *Prosopis* spp. germ (Lamarque et al. 1994; Sciammaro 2015). Interestingly, based on almost identical FA profiles, *P. alba* and *P. nigra* exhibit a strict taxonomical parentage, in agreement with the similarity assessed through the polyphenol patterns (Picariello et al. 2017). *P. ruscifolia* and *C. siliqua* FA profiles were characterized by minor differences. More in detail, the germ from European carob (*C. siliqua*) had a less heterogeneous FA profile, due to a very low-amount or very long-chain FAs (C20–C24), which, in *P. alba* and *P. nigra*, exceed 6–7%. In *P. ruscifolia* SGF, C20–C24 FA occurred at an intermediate level between *C. siliqua* and *P. alba*/*P. nigra*. Moreover, *C. siliqua* SGF contained significantly higher amounts of monounsaturated FA (MUFA), whereas it was lower in total polyunsaturated FA (PUFA) than the *Prosopis* counterparts. It has been underlined that although the figures appear clearly different among different species, data should be statistically validated over a higher number of biological replicates.

Because of the high concentration of PUFA, algarrobo and carob SGF can supply nutritionally valuable essential ω-6 FA, which, on the other hand, are susceptible of auto-oxidation, thereby affecting the stability of flour and shelf life of derived products. The lipid fraction of *Prosopis* spp. SGF is also interesting as a potential source of very long-chain FAs, which exert health-promoting effects in humans (Abedi and Sahari 2014). Very long-chain FAs are rather rare in most of the foods ordinarily consumed and have been extensively studied because of the intense biosynthetic activity in developing seeds and for the capability to confer the entire lipid fraction with plastic properties. By a nutritional standpoint, very long-chain FAs serve as a precursor of important lipid signaling mediators and are supposed to play pivotal roles in a number of physiopathological pathways (Lee et al. 2015). On the other hand, SGF is poor in linolenic acid (C18:3, ω-3), which was lower than 2% in all the cases, although *Prosopis* spp., mainly *P. alba* and *P. nigra*, contain almost twofold the amount of *C. siliqua*.

Unsaponifiable Fraction

Phytosterols are natural constituents of plant-based foods, which have been shown to lower total serum cholesterol and low-density lipoprotein. The most common phytosterols detected in SGF samples by GC-FID analysis, including campesterol, β-sitosterol, stigmasterol, and Δ_5-avenasterol, are quantified in Table 1. β-Sitosterol was the dominant phytosterol in SGF (concentration range 419.2–732.6 mg/kg), with particularly high figures in *C. siliqua*. Brassicasterol was not detected in any of the SGF samples. In partial agreement with the FA profiles, phytosterols reflect the taxonomic similarity between *Prosopis* varieties and the differences with *C. siliqua*.

Squalene and α- and β + α-tocopherol were quantified in the unsaponifiable lipid fraction of SGF (Table 1), whereas δ-tocopherol and tocotrienols did not occurred at detectable

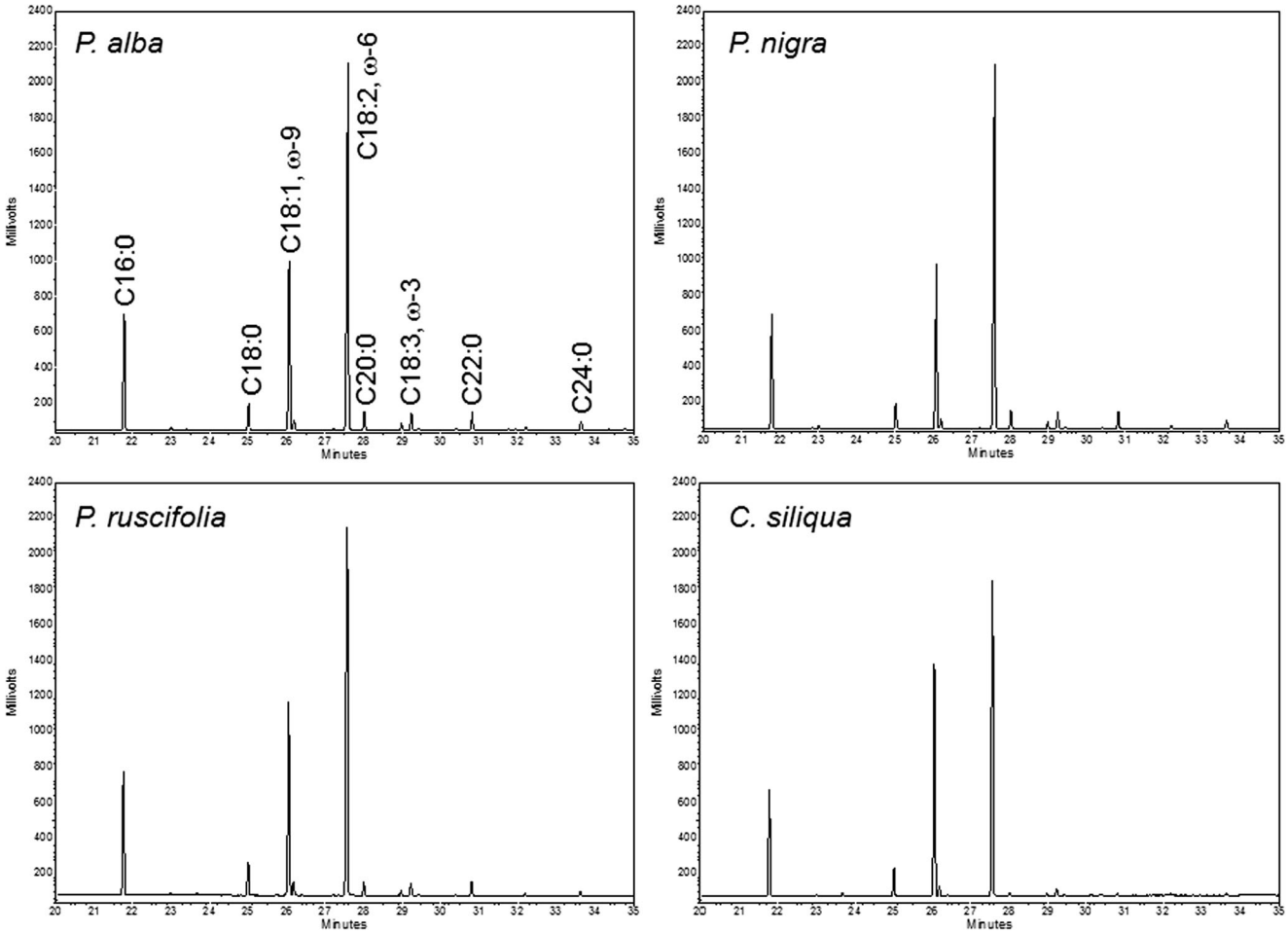

Fig. 1 GC-FID comparison of FAME from *Prosopis* spp. and *C. siliqua* SGF glycerolipids

amount. The amount of squalene and tocopherols was not particularly high, compared to the lipid fractions of other plant seeds (Ryan et al. 2007).

MALDI-TOF MS Analysis of SGF Lipids

In the analysis of FA with conventional GC-based methods, the information about the parent glycerolipid is lost, due to hydrolysis and trans-esterification. Direct MS of intact lipids enables the access to such information, which, in many cases, is crucial to establish the possible presence of partial acylglycerols (mono/diacylglycerols) or PLs. MALDI-TOF MS techniques have emerged as very advantageous strategies for the rapid and specific profiling of intact lipids in complex mixtures, providing analytical responses comparable to those obtained by direct flow injection electrospray MS, also referred to as shotgun lipidomics (Fuchs et al. 2010). The advantages of MALDI-TOF MS in the analysis of intact lipids include (i) minimal sample handling and no derivatization steps; (ii) very fast analysis (seconds-few minutes range); (iii) relative tolerance to interfering compounds; (iv) sensitivity, specificity, and high dynamic range; and (v) straightforward interpretation of results (Picariello et al. 2009, 2010). The MALDI-TOF mass spectra of the entire lipid extract from SGF samples are compared in Fig. 2, where TAGs, detected exclusively as Na^+ adducts, are assigned through the total carbon number (CN) of acyl chains and the number of unsaturated ones.

The MALDI-MS spectra also showed prominent signals attributable of PL, especially PC, with intensity comparable to those of TAG. In MS analyses, PC exhibits a much higher ionization efficiency if compared to neutral lipids, especially when dissolved at acidic pH, because of its zwitterionic nature. The mutual interference between PL and TAG hampers a straightforward detection of the respective families of compounds. For this reason, PL and TAG were fractionated using HAP chromatography (Pinto et al. 2014) prior to MALDI-TOF MS analysis of the individual classes of compounds. The spectrum of isolated TAG species (Fig. 3) clearly showed that the non-polar lipid fraction was dominated by the C54 TAG cluster, the C54:4 (MW 905.8, as Na^+ adducts) and C54:5 (MW 903.8), producing the most intense signals in all the SGF samples. Significant amounts of oxidized TAG (ox-TAG, MW 919.8 and 921.8) also occurred at variable

Table 1 Fatty acid (% of total) and unsaponifiable fraction composition of lipids from *Prosopis* spp. and *C. siliqua* seed germ flour

	P. alba	*P. nigra*	*P. ruscifolia*	*C. siliqua*
Fatty acid (area %)				
Palmitic, C16:0	13.93 ± 0.55	13.95 ± 0.73	14.73 ± 0.88	14.12 ± 0.65
Palmitoleic, C16:1	0.34 ± 0.10	0.33 ± 0.11	0.34 ± 0.10	0.20 ± 0.09
Heptadecanoic, C17:0	0.11 ± 0.01	0.11 ± 0.01	0.09 ± 0.01	0.17 ± 0.02
Stearic, C18:0	3.08 ± 0.24	3.11 ± 0.19	4.00 ± 0.22	3.71 ± 0.23
Oleic, C18:1, ω-9*c*	21.17 ± 1.01	21.48 ± 1.10	23.85 ± 0.98	32.01 ± 1.22
Linoleic, C18:2, ω-6*c*	50.56 ± 2.57	50.23 ± 2.54	46.96 ± 2.15	43.27 ± 2.23
Arachidic, C20:0	2.06 ± 0.88	2.08 ± 0.45	1.64 ± 0.37	0.44 ± 0.11
cis-11-Eicosenoic, C20:1	0.77 ± 0.05	0.78 ± 0.08	0.60 ± 0.04	0.29 ± 0.03
Linolenic, C18:3, ω-3	1.97 ± 0.25	1.90 ± 0.21	1.41 ± 0.19	0.96 ± 0.15
Behenic, C22:0	2.04 ± 0.18	2.06 ± 0.15	1.80 ± 0.16	0.26 ± 0.08
Lignoceric, C24:0	1.02 ± 0.23	1.05 ± 0.25	0.72 ± 0.17	0.26 ± 0.06
Σ-SFA	22.24 ± 1.09	22.36 ± 0.89	22.98 ± 1.00	18.96 ± 0.68
Σ-MUFA	22.28 ± 1.01	22.59 ± 1.11	24.79 ± 0.98	32.50 ± 1.22
Σ-PUFA	52.53 ± 2.58	52.13 ± 2.78	48.37 ± 2.58	44.23 ± 2.23
Σ-PUFA/Σ-SFA	2.36	2.33	2.10	2.33
Unsaponifiable (mg/kg)				
Squalene	1.80 ± 0.15	5.68 ± 1.02	5.83 ± 1.00	3.39 ± 0.84
α-Tocopherol	–	39.64 ± 6.54	46.67 ± 5.48	14.84 ± 2.24
β + γ-Tocopherol	13.90 ± 4.25	14.42 ± 2.21	22.67 ± 3.56	36.76 ± 2.45
Brassicasterol	–	–	–	–
Campesterol	116.62 ± 12.56	97.08 ± 9.87	116.54 ± 11.58	61.67 ± 3.18
Stigmasterol	169.28 ± 24.63	170.76 ± 27.15	172.22 ± 26.34	140.83 ± 12.45
β-Sitosterol	419.24 ± 38.74	450.00 ± 42.98	440.63 ± 39.48	736.62 ± 36.84
Δ_5-Avenasterol	26.15 ± 2.65	14.96 ± 2.00	34.22 ± 23.88	77.40 ± 9.25

intensity, most likely due to auto-oxidation of polyunsaturated acyl chains during germ milling or flour storage. The auto-oxidation events were also confirmed by a series of low-intensity signals at *m*/*z* 769–815 arising from β-scission of acyl chains in TAG (Picariello et al. 2009). Remarkably, SGF from *Prosopis* spp. contained significant amounts of TAG with very high CN, including C56–C60, which were missing in the extract of *C. siliqua*, reflecting the relatively high content of very long-chain FA in *Prosopis* germ samples, as already emphasized by GC analysis of FA (Table 1). Low-intensity signals of diacylglycerols (DAGs), due to incomplete biosynthesis of TAG, were observed in all the samples (e.g., DAG C36:3 at *m*/*z* 641.5). The similarity among lipid profiles was consistent with the phylogenetic relationship at a family

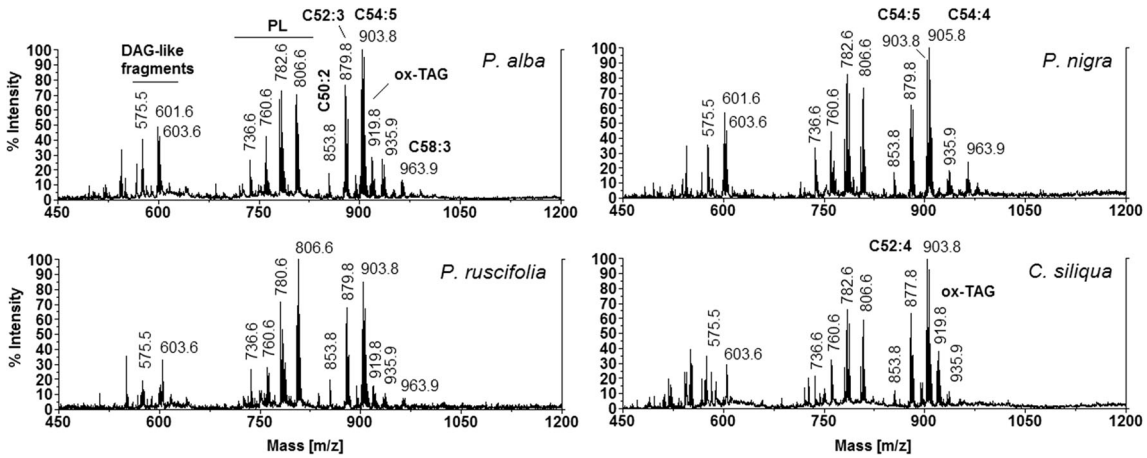

Fig. 2 Comparative MALDI-TOF MS analysis of intact lipids extracted from *Prosopis* spp. and *C. siliqua* SGF samples. Some of the most representative lipid components or lipid classes are assigned

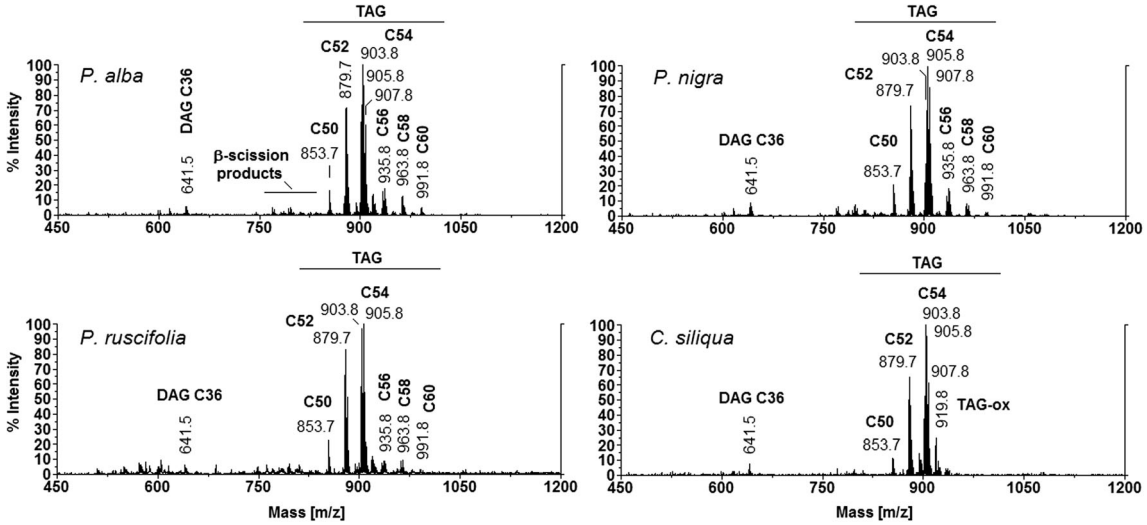

Fig. 3 MALDI TOF mass spectra of the flow-through resulting from separation with hydroxyapatite chromatography. The spectra clearly show TAG and DAG purified from *Prosopis* spp. and *C. siliqua* SGF, without the interference from phospholipids

level between *C. siliqua* and *Prosopis* spp. and at an intra-genus level among the *Prosopis* congeners.

The exemplificative mass spectrum of fractionated PL from *P. alba* acquired in the positive ion mode is shown in Fig. 4, along with the tentative assignment of the main PL signals. The PL profile of the other samples did not exhibit significant differences (not shown). Practically, PC and corresponding lyso-phosphatidylcholines (LPCs) produced very intense signals, as both protonated and Na^+ adducts, although other PL classes, including phosphatidylethanolamine (PE) and phosphatidylinositol (PI), also occurred at detectable amount. PC dominated the mass spectra of PL families even when the MALDI-TOF MS analysis was carried out in the negative ion mode (not shown), using 9-aminoacridine as the matrix

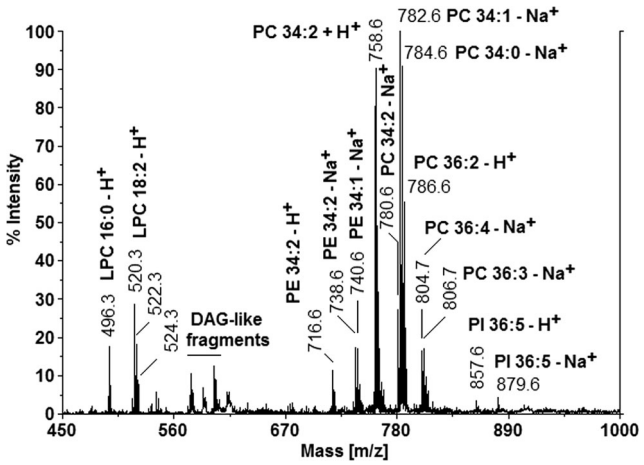

Fig. 4 Exemplificative MALDI-TOF mass spectrum of phospholipids from *P. alba* SGF purified by hydroxyapatite chromatography. The most intense signals are tentatively assigned to phosphatidylcholine (PC), phosphatidylethanolamine (PE), and phosphatidylinositol (PI) compounds. The PL fraction from the other samples did not show significant differences (not shown)

to balance the efficiency to ionization of the different PL families (Fuchs et al. 2010).

ATR-FTIR Quantitation of PL in SGF Lipids

Due to the compound-dependent ionization efficiency, MALDI-MS analysis did not enable a direct quantitative correlation between different classes of lipid species.

A gross quantification of PL in SGF lipid extracts was obtained by ATR-FTIR spectroscopy, based on PL-specific absorption bands in the 1300–970 cm^{-1} IR range, attributed to phosphate diester (PO^{2-}) stretch and symmetric/asymmetric ester C-O-P stretch, which are missing in the spectra of TAG and other non-phosphate-containing lipids. These bands have been already exploited to quantify total PL in vegetable oils (Nzai and Proctor 1998; Meng et al. 2014) and dietary supplements (Kuligowski et al. 2008), with very good accuracy and sensitivity. A calibration curve was generated with standard PC in pure triolein at varying relative concentrations (1, 5, 10, 20, and 50% *v*/*v* of PC in equimolar solution of triolein). ATR-FTIR spectra of standard mixtures are shown in the upper panel of Fig. 5 along with an exemplificative spectrum of SGF lipids from *P. alba* (red line). By comparison among spectra, it appears evident the increasing of absorption bands at 1084 and 1063 cm^{-1} with the increment of relative PL amount. Although the bands centered at 1243 and 1167 cm^{-1} are also specific of phosphate-containing lipids, those at 1084 and 1063 cm^{-1} were better correlated with the PL amount, in line with the findings of other authors (Nzai and Proctor 1998). Therefore, the bands at 1084 and 1063 cm^{-1} were selected for the approximate quantitative determination of PL in SGF lipid extracts.

Software-assisted normalization and integration of diagnostic 1084–1063 cm^{-1} PL bands were performed on the

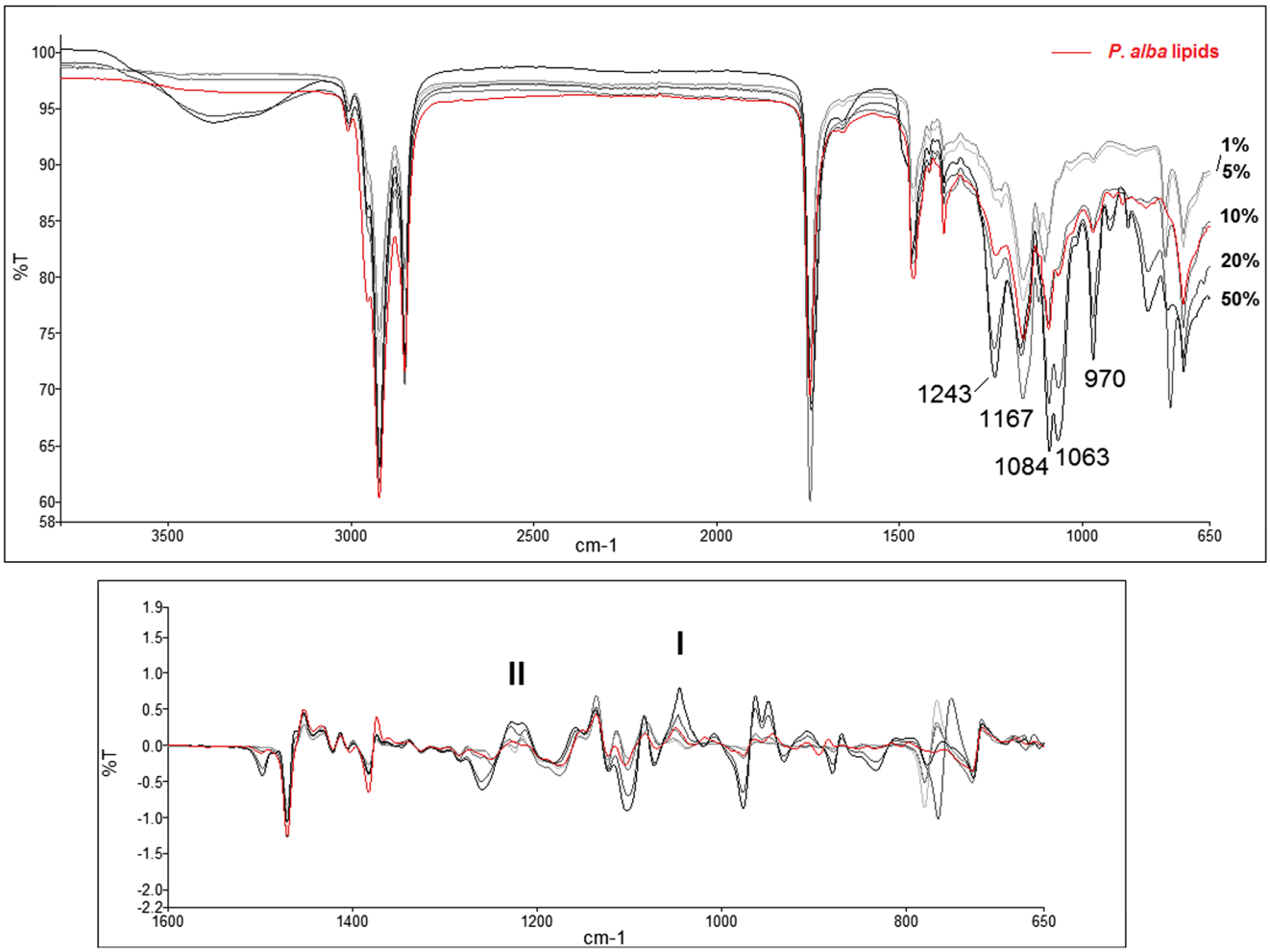

Fig. 5 *Upper panel*: ATR-FTIR spectra of standard mixtures at varying percentages of pure PC in triolein. The spectrum of lipids from *P. alba* SGF (red line was taken as an exemplificative test sample). *Lower panel*: first-order derivative ATR-FTIR spectra. The band centered at 1044 cm^{-1} (band I), arising from phosphate-containing groups, was selected for the quantification of PL in lipid extracts of SGF samples

first-order derivative differential spectra (band I, Fig. 5, lower panel), which yielded a sharp band centered at 1044 cm^{-1} embracing the two partially overlapped bands and provided the highest regression correlation factor: $R^2 = 0.87$. The 1044 cm^{-1} band area of PL in test samples was related to the PC concentration in the standard curve.

A series of additional bands could be attributed to PL groups in the fingerprinting region (e.g., P=O vibration in the 1300–1250 cm^{-1} range, Fig. 5, upper panel), but they overlapped with C–O–C vibration bands of co-extracted TAG and were less specific (Nzai and Proctor 1998). Alternatively, the asymmetric phosphate diester (PO^{2-}) stretch at 1243 cm^{-1} as the second-order derivative spectra can been used with good accuracy and quantitative results comparable to those obtained from integration of 1084–1063 cm^{-1} bands (Meng et al. 2014). However, in our case, the band at 1243 cm^{-1} was poorly resolved in both the first-order and second-order derivative spectra and it was not straightforwardly integrated (band 2, Fig. 5, lower panel). A sharp band at 970 cm^{-1} in the raw spectra (Fig. 5, upper panel) arose from C–N asymmetric stretching of quaternary ammonium groups. Thus, this latter band is usually suitable for determining only the content of PC, but it tends to underestimate the entire PL content. For these reasons, the band area at 1044 cm^{-1} for SGF lipid extracts was considered the most suitable to calculate the PL percentage, using the regression equation obtained with standard mixtures.

The estimated content of PL in the SGF lipid fraction was 9.5% (*w*/*w*) for *C. siliqua*, while PL content in *Prosopis* SGF was slightly higher, being 10.5, 10.8, and 11.8% in *P. alba*, *P. nigra*, and *P. ruscifolia*, respectively.

Possible Functional and Technological Role of Lipids in *Prosopis* spp. and *C. siliqua* Seed Germ Flour

Phospholipids have been used to prevent oxidation of oils and several food matrices. Except for the cases of rich metal ion-meat and dehydrated lipid matrices, in which they act as pro-

oxidants, phospholipids have intrinsic antioxidant properties (Cui and Decker 2016). The relatively high content of PL can justify the antioxidant potential of SGF, complementing that of polyphenol compounds. Besides having key nutritional properties, lipids have primary impact of the food technology of dough. Specifically, in bread-making process, lipids distribute into different phases of dough, reducing the interfacial energy. Expansion of dough during fermentation depends on the formation of air-containing cells surrounded by liquid film lamellae and englobed in a viscoelastic gluten-starch network. Carbon dioxide produced by yeast fermentation can only diffuse into preexisting air cells, affecting the loaf volume and the quality of bread (Pareyt et al. 2011). Two processes contribute to stabilize gas cells in dough: hardening of the gluten-starch matrix where cells are inserted in and the presence of surface-active components in the interfacial film, such as proteins, polar lipids, or surfactants that are able to form condensed monolayers (Selmair and Koehler 2010).

Generally, phospholipids or glycolipids, the latter recently described in the hydro-alcoholic extracts of *Prosopis* spp. and *C. siliqua* SGF (Picariello et al. 2017), act as effective emulsifiers, affecting dough handling, as well as structural and sensorial properties of baked products (Pareyt et al. 2011). In this sense, the most common is lecithin that, in controlled amounts, improves the fermentation behavior of yeast dough, loaf volume, and crumb structure and contributes to delay bread staling. By virtue of their relatively high content, polar lipids are expected to positively affect the baking properties of carob and algarrobo SGF either as a pure flour ingredient or in combination with other baking flours. Furthermore, in the presence of an enzymatically regulated complex redox system, such as gluten-containing and gluten-free flours, lipids can contribute to the formation of a protein network, characterized by covalent inter-chain linkages.

Thus, when blended with wheat flour, SGF might contribute to improve bread and baked products in both technological and nutritional terms. On the other hand, through opportune combinations with gluten-free flours, SGF could modulate the properties of baked commodities destined to individuals with celiac disease.

Conclusions

The flour of *Prosopis* spp. and *C. siliqua* seed germ presents a nutritionally and technologically interesting lipid profile, which was characterized with a multiplexed analytical approach. In addition to prominent levels of poly- and monounsaturated FA, *Prosopis* spp. germ also contains relatively high amounts of C20–C24 FA, which could exert a number of health-promoting actions in humans, especially ameliorating the metabolic profile of blood lipids. *Prosopis* and *C. siliqua* seed germ is relatively high in PL, which contribute to prevent oxidation of oils and act as emulsifiers in baking flour. In the case of breads, PLs are known to interact with flour components, enhancing structure during mixing and improving yeast fermentation of dough. Overall, PLs contribute to prepare high-quality baked products with increased loaf volume, soft crumb structure, good sensory attributes, and delayed bread staling.

Thus, also in consideration of a peculiar protein and polyphenolic composition, carob and algarrobo SGF is a promising raw material, obtained from processing by-products of neglected crops, to prepare gluten-containing or gluten-free baked products endowed with excellent sensory properties and potential health-promoting benefits.

Acknowledgements The present investigation has been carried out in the framework of the CNR/CONICET (Italy/Argentina) bilateral research agreement 2015–2016 awarded to G. M. and M. C. P.

Compliance with Ethical Standards

Conflict of Interest The authors declare that they have no competing interests.

Ethical Approval This article does not contain any studies with human participants or animals performed by any of the authors.

Informed consent Not applicable

References

Abedi E, Sahari MA (2014) Long-chain polyunsaturated fatty acid sources and evaluation of their nutritional and functional properties. Food Sci Nutr 2(5):443–463

Association of Official Analytical Chemists (AOAC). (2001) Official Method 996.06. In: Official methods of analysis, 17th ed., revised; AOAC: Gaithersburg

Avallone R, Plessi M, Baraldi M, Monzani A (1997) Determination of chemical composition of carob (Ceratonia siliqua): protein, fat, carbohydrates, and tannins. J Food Compost Anal 10(2):166–172

Ayaz FA, Torun H, Ayaz S, Correia PJ, Alaiz M, Sanz C et al (2007) Determination of chemical composition of anatolian carob pod (*Ceratonia siliqua* L.): sugars, amino and organic acids, minerals and phenolic compounds. J Food Quality 30:1040–1055

Bahrami N, Yonekura L, Linforth R, Carvalho da Silva M, Hill S, Penson S, Chope G, Fisk ID (2014) Comparison of ambient solvent extraction methods for the analysis of fatty acids in non-starch lipids of flour and starch. J Sci Food Agric 94(3):415–423

Batista MT, Gomez ET (1993) C-glycosylflavones from Ceratonia siliqua cotyledons. Phytochemistry 34:1191–1193

Caligiani A, Bonzanini F, Palla G, Cirlini M, Bruni R (2010) Characterization of a potential nutraceutical ingredient: pomegranate (*Punica granatum* L) seed oil unsaponifiable fraction. Plant Foods Hum Nutr 65:277–283

Cattaneo F, Costamagna MS, Zampini IC, Sayago J, Alberto MR, Chamorro V, Pazos A, Thomas-Valdés S, Schmeda-Hirschmann G, Isla MI (2016) Flour from Prosopis alba cotyledons: a natural source of nutrient and bioactive phytochemicals. Food Chem 208:89–96

Choge SK, Pasiecznik NM, Harvey M, Wright J, Awan SZ, Harris PJC (2007) *Prosopis* pods as human food, with special reference to Kenya. Water SA 33:419–424

Cui L, Decker EA (2016) Phospholipids in foods: prooxidants or antioxidants? J Sci Food Agric 96(1):18–31

Custódio L, Escapa AL, Fernandes E, Fajardo A, Aligué R, Alberício F, Neng N, Nogueira JMF, Romano A (2011) Phytochemical profile, antioxidant and cytotoxic activities of the carob tree (*Ceratonia siliqua* L.) germ flour extracts. Plant Foods Hum Nutr 66(1):78–84

Dakia PA, Wathelet B, Paquot M (2007) Isolation and chemical evaluation of carob (*Ceratonia siliqua* L.) seed germ. Food Chem 102: 1368–1374

Dakia PA (2011) Carob (*Ceratonia siliqua* L.) seeds, endosperm and germ composition, and application to health. In: Preedy VR, Watson RR, Patel VB (eds) Nuts and seeds in health and disease prevention. Chap. 35. Elsevier, Academic, New York, pp 293–299

Fuchs B, Bischoff A, Süss R, Teuber K, Schürenberg M, Suckau D, Schiller J (2009) Phosphatidylcholines and -ethanolamines can be easily mistaken in phospholipid mixtures: a negative ion MALDI-TOF MS study with 9-aminoacridine as matrix and egg yolk as selected example. Anal Bioanal Chem 395(8):2479–2487

Fuchs B, Süss R, Schiller J (2010) An update of MALDI-TOF mass spectrometry in lipid research. Prog Lipid Res 49(4):450–475

Kuligowski J, Quintás G, Garrigues S, de la Guardia M (2008) Determination of lecithin and soybean oil in dietary supplements using partial least squares-Fourier transform infrared spectroscopy. Talanta 77(1):229–234

Lamarque AL, Maestri DM, Grosso NR, Zygadlo JA, Guzmán CA (1994) Proximate composition and seed lipid components of some *Prosopis* (leguminosae) from Argentina. J Sci Food Agric 66:323–326

Lee YS, Cho Y, Shin M-J (2015) Dietary very long chain saturated fatty acids and metabolic factors: findings from the Korea National Health and Nutrition Examination Survey 2013. Clin Nutr Res 4: 182–189

Li H, Song F, Xing J, Tsao R, Liu Z, Liu S (2009) Screening and structural characterization of α-glucosidase inhibitors from hawthorn leaf flavonoids extract by ultrafiltration LC-DAD-MSn and SORI-CID FTICR MS. J Am Soc Mass Spectrom 20:1496–1503

Meng X, Ye Q, Pan Q, Ding Y, Wei M, Liu Y, van de Voort FR (2014) Total phospholipids in edible oils by in-vial solvent extraction coupled with FTIR analysis. J Agric Food Chem 62:3101–3017

Nzai JM, Proctor A (1998) Determination of phospholipids in vegetable oil by Fourier transform infrared spectroscopy. J Am Oil Chem Soc 75:1281–1289

Pareyt B, Finnie SM, Putseys JA, Delcour JA (2011) Lipids in bread making: sources, interactions, and impact on bread quality. J Cereal Sci 542:266–279

Pérez MJ, Cuello AS, Zampini IC, Ordoñez RM, Alberto MR, Quispe C, Schmeda-Hirschmann G, Isla MI (2014) Polyphenolic compounds and anthocyanin content of *Prosopis nigra* and *Prosopis alba* pods flour and their antioxidant and anti-inflammatory capacities. Food Res Int 64:762–771

Phillips KM, Ruggio DM, Ashraf-Khorassani M (2005) Phytosterol composition of nuts and seeds commonly consumed in the United States. J Agric Food Chem 53:9436–9445

Picariello G, Paduano A, Sacchi R, Addeo F (2009) MALDI-TOF mass spectrometry profiling of polar and nonpolar fractions in heated vegetable oils. J Agric Food Chem 57(12):5391–5400

Picariello G, Romano R, Addeo F (2010) Nitrocellulose film substrate minimizes fragmentation in matrix-assisted laser desorption ionization time-of-flight mass spectrometry analysis of triacylglycerols. Anal Chem 82:5783–5791

Picariello G, Sciammaro L, Siano F, Volpe MG, Puppo MC, Mamone G (2017) Comparative analysis of C-glycosidic flavonoids from *Prosopis* spp. and *Ceratonia siliqua* seed germ flour. Food Res Int 99:730–738

Pinto G, Caira S, Mamone G, Ferranti P, Addeo F, Picariello G (2014) Fractionation of complex lipid mixtures by hydroxyapatite chromatography for lipidomic purposes. J Chromatogr A 1360:82–92

Ryan E, Galvin K, O'Connor TP, Maguire AR, O'Brien NM (2007) Phytosterol, squalene, tocopherol content and fatty acid profile of selected seeds, grains, and legumes. Plant Foods Hum Nutr 62:85–91

Saunders RM, Becker R (1989) Development of *Prosopis* species leguminous trees as an agricultural crop. In: Wickens GE, Haq N, Day PR (eds) New crops for food and industry. Chapman and Hall University Press, Cambridge

Sciammaro L (2015) Physicochemical characterization of algarrobo pods and flours (*Prosopis alba* and *Prosopis nigra*). Applications on baked and fermented products. Ph.D Thesis. UNLP, La Plata, Argentina.

Sciammaro L, Ferrero C, Puppo MC (2016) Chemical and nutritional properties of different fractions of Prosopis alba pods and seeds. J Food Meas Charact 10:103–112

Selmair PL, Koehler P (2010) Role of glycolipids in breadmaking. Lipid Technol 22:7–10

Siano F, Straccia MC, Paolucci M, Fasulo G, Boscaino F, Volpe MG (2016) Physico-chemical properties and fatty acid composition of pomegranate, cherry and pumpkin seed oils. J Sci Food Agric 96: 1730–1735

Smith BM, Bean SR, Schober TJ, Tilley M, Herald TJ, Aramouni F (2010) Composition and molecular weight distribution of carob germ protein fractions. J Agric Food Chem 58:7794–7800